RSC Advances

ROYAL SOCIETY OF CHEMISTRY

www.rsc.org/advances

Journal Name

RSCPublishing

ARTICLE

Cite this: DOI: 10.1039/xoxxoooooox

Microwave-assisted Synthesis of Novel Julolidinyl-Based Nonlinear Optical Chromophores with Enhanced Electro-optic Activity

Received ooth January 2012,
Accepted ooth January 2012

DOI: 10.1039/xoxxoooooox

www.rsc.org/

Airui Zhang, [a,b] Hongyan Xiao, [a] Chengcheng Peng, [a,b] Shuhui Bo, *[,a] Huajun Xu, [a,b] Maolin Zhang, [a,b] Guowei Deng, [a,b] Zhen Zhen, *[,a] Xinhou Liu [a].

Under microwave (MW) irradiation at proper temperature, three chromophores (**A**, **B**, **C**) with julolidinyl-based donors and TCF or CF_3-Ph-TCF acceptors have been synthesized in high overall yields compared with the conventional heating method. The introduction of MW heating approach in the synthesis of these chromophores was proved to markedly shorten reaction times, reduce by-products and increase the efficiency. The solvatochromic behavior and cyclic voltammetry (CV) measurements suggested that chromophores **B** and **C** with stronger acceptor can be more easily polarized with respect to chromophore **A**. The solvent dependence of the relevant theoretically parameters including dipole moment (μ), first-order polarizability (α), hyperpolarizability (β) and bond-length alternation (BLA) of all chromophores were also studied by DFT calculations. All these chromophores showed good thermal stability and large β values. In electro-optic (EO) activities test, guest-host poled polymer **A/APC** exhibited the highest EO coefficient (r_{33}) of 192 pm/V at 1.31 μm. The MW-assisted syntheses and systematic analyses afforded a rational design for NLO chromophores, and provided a new method to optimize the structures of the chromophores to achieve higher r_{33} values.

Introduction

Electro-optic (EO) materials especially organic EO materials have been attracting considerable attention due to their great potential over conventional inorganic crystalline materials for novel photonic applications.[1-3] Some of them with high EO activities and ultrafast response time have been used to fabricate the high-speed optical waveguide devices,[4, 5] such as Mach-Zehnder and phase modulators with half-wave voltage lower than 1 V.[6, 7] In order to obtain the macroscopic EO responses, materials must have noncentrosymmetrical structure and show fine microscopic nonlinear optics (NLO) properties, good chemical-, thermal-, photochemical stabilities as well as low optical loss.[2, 5, 8, 9] As potential building blocks in EO devices, lots of push-pull type NLO chromophores with various structures showing large hyperpolarizability (β) and dipole moments (μ) have been designed and synthesized.[10-17] Among them, CLD-type chromophores (containing the isophorone-derived tetraene bridges) with terminal 2-dicyanomethylene-3-cyano-4,5,5-trimethyl-2,5-dihydrofuran (TCF) or 2-dicyanomethylene-3-cyano-4-methyl-5-phenyl-5-trifluoromethyl-2,5-dihydrofuran (CF_3-Ph-TCF) acceptor were widely investigated due to their large β and good utility for EO devices.[18-22] They represented one of the most useful and effective frameworks and have been used as the core building block for some novel developed EO materials that yield excellent NLO response and good processibility.[21, 23-28] However, due to the poor Knoevenagel condensation reactivity, the CLD-type chromophores and configurationally locked polyene (CLP) crystals were obtained in low yield and the synthesis procedures were tedious and time-consuming.[23, 29-31] Thus, further improvement of the properties of these materials and the synthetic methods need to be focused on.

Julolidinyl-based group as the electron donor has been reported with better solubility, stronger electron-donating ability and larger steric hindrance than the classical dimethylanilino moiety.[32-35] Chromophores with julolidinyl-based donor and TCF acceptor with large EO coefficients (r_{33}) and good stabilities have been studied in our groups.[36, 37] However, chromophore with CLD-type bridge end-capped with julolidinyl-based donor and CF_3-Ph-TCF acceptor, showed a dramatically decreased r_{33} (~20 pm/V at 1.31 μm).[18] Presumably because of the poor performance (decreased EO property and the inefficient poling), this julolidinyl-based CLD-type chromophores have not been extensively used in EO materials and devices.

Microwave-assisted organic synthesis (MAOS)[38-40] was widely recognized as an effective reaction protocol, which can circumvent the need for prolonged heating and result in rapid, clean and high-yielding transformations. Application of MW

irradiation for the substitution and condensation reaction is a hotspot that was successfully demonstrated.[41, 42] Up to now, dipolar polarization and conduction mechanism are the two major mechanisms in chemical reaction systems, resulting in the high final temperature and reaction efficiency.[41, 43, 44] Liu et al.,[45] for the first time, introduced the MW methodology in the NLO field to control the synthesis of a series of TCF-based acceptors. From then on, few articles were reported the MW organic reactions in the synthesis of CLD-type chromophores.[45, 46] Herein, the MAOS method is employed to synthesize the highly active chromophores with julolidinyl-based donors and TCF or CF_3-Ph-TCF acceptors that linked together via the isophorone-based bridge (**A, B** and **C** in Scheme 1). The encouraging discovery was that the overall yield of the chromophore **A** increased from 14.4% to 26.7% simply by replacing three conventional oil bath heating steps with MW energy heating. The UV-Vis-NIR absorption spectra and DFT calculations suggested that these chromophores can be easily polarized and have more attractive linear and nonlinear optical performance. The hyperpolarizability of chromophore **A** with weak acceptor increased with the increase of the solvent polarity,which was different to that of chromophores **B** and **C** with strong acceptor. Also, all the chromophores were soluble in common solvents and showed good thermal stability. When chromophores **A, B** and **C** were doped in the amorphous polycarbonate (**APC**) polymers, the obtained EO polymer exhibited good film-forming ability. Excitingly, the guest-host EO polymer doping 20 wt% of the novel chromophore **A** with TCF acceptor has been poled to afford the large r_{33} value (192 pm/V at 1.31μm), while chromophores **B** and **C** with stronger CF_3-Ph-TCF acceptor showed the low r_{33} value (24 pm/V).

Results and Discussion

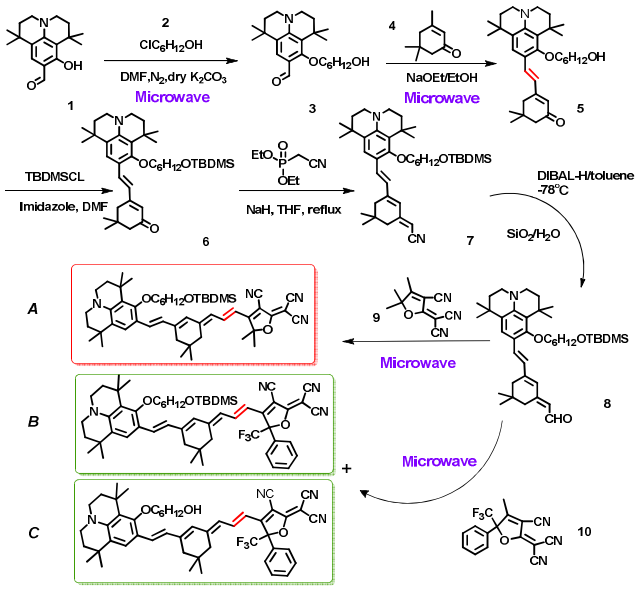

Scheme 1. Synthesis route of the chromophores **A**, **B** and **C**

Synthesis. Because the MW methodology provides an efficient reaction outcome for the substitution and condensation reactions to study the MW heating effect, three steps used MW heating in place of the conventional heating. In the reaction between compound **1** and **2** (Scheme 1) under MW heating, the reaction time was shortened to less than one hour and the yield was improved from 73% to 82% compared with the conventional heating. Furthermore, the temperature (130 °C) and the solvent (DMF) of MW reaction were the same as that of conventional heating. To reveal the effect of the temperature, this reaction was heated under MW irradiation at the temperature around 155~160 °C. And the yield was almost the same after improving the temperature higher than the boiling point of the solvents. It was probably due to the fact that the substrates or ions presented in the solvent would facilitate the formation of 'boiling nuclei' in this solution system, leading to the dropped temperature to the normal boiling point of the solvent.

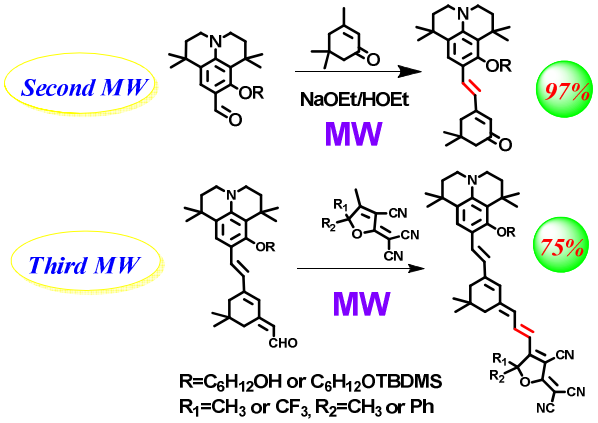

Scheme 2 MAOS of the second & third MW reaction。

Knoevenagel condensation between compound **3** and **4** was separately conducted under conventional and MW heating conditions to demonstrate the specific microwave effect. As the two mechanisms mentioned previously polar solvents and ions were reported necessary for MW heating to accelerate the MW reaction.[41] Thus, solvents with higher dielectric constant will make it easier to absorb the MW irradiation and result in higher reactive temperature. With the increase of solvent polarity, the polarity of molecule increased from the ground state to the transition state. It suggested a decreased activation energy resulting in an enhancement of reactivity.[43] Fortunately, ethanol could couple better with MW irradiation and resulted in a more repaid temperature increase.[41] In conventional heating, the ethanol was the common solvent and the sodium ethoxide was used to provide the alkaline environment to effectively promote the condensation. In MW heating, on the other hand, the ethanol was chose as polar solvent and sodium ethoxide was used as ions to facilitate the reaction according to the mechanisms mentioned above. The reaction proceeded within 5 hours under conventional heating (refluxing in ethanol solution) to give a moderate yield (about 60%). However, it could afford compound **5** in 97% yield (Scheme 2) for only several minutes under MW heating. The optimized irradiation time and heating temperature were 30 min and 120 °C, respectively. With extending the heating time and increasing the heating temperature for MW method, the yield decreased a little. This may be attributed that the longer reaction time and the higher temperature could lead to the decomposition of products. In this respect, MW heating made this reaction time shorter and heating temperature higher than that of conventional heating. This heating temperature was proved to be higher than the boiling point of the ethanol solvent, which was the so-called 'superheating effect'.[41] It was supposed to raise the boiling point here due to the conduction mechanism. The ions in the solutions, under the electric field of MW, would move through

the solution faster and collide with each other more frequently, resulting in a rapid temperature increase.

The bulky *tert*-butyldimethylsilyl (TBDMS) group was introduced to protect the hydroxyl group, improve the solubility and provide a suitable shape isolation to weaken the dipole-dipole interaction for higher poling efficiency. The following steps are Wittig-Horner reaction using diethyl cyanomethylphosphonate and DIBALH involved reduction. The dienone **6** was then converted to trienal **8** in good yield by this two-step route shown in Scheme 1. This route has been previously reported to synthesize the trienal analogues.[23]

Table 1 Methods for the final reaction of chromophore **A**.

	Time[a] (min)	Temp[b] (°C)	Yield (%)	Sol[c]
MH	40	85	75	EtOH
CH	360	90	55	EtOH

[a] The irradiation time. [b] The reaction temperature. [c] The solvent we used in the reaction. MH: MW heating. CH: conventional heating.

The final Knoevenagel condensation was the reaction between donor-bridge **8** and the strong acceptor **9** or **10** to form chromophores **A**, **B** and **C** (Scheme 2). As shown in Table 1, through the focused MAOS, the compound **8** was easily condensed with acceptor **9**. The yield of chromophore **A** was improved to 75% and the reaction time was shortened to 40 min compared with conventional heating, respectively. MAOS was then supposed to be a better method in improving the yield of chromophores **B** and **C**. Controlling the irradiation time can adjust the ratio of the chromophores **B** and **C**. The longer time MW irradiated, the less **B** containing TBDMS groups was obtained. But it was mainly observed when the chromophores used CF_3-Ph-TCF as the acceptor. We speculated that the silicon-oxygen bond (Si-O) in chromophore **B** tended to be ionic and easy to break under the MW irradiation. Above all, MAOS method exhibited several advantages over the conventional heating, including the significant shortened reaction time, the improvement of yield and the reduced side reactions in the process for easier purification. Structures of chromophores **A, B** and **C** were confirmed by ^1H and ^{13}C NMR and MALDI-TOF-MS.

Table 2. UV-Vis-NIR absorptions for chromophores A, B and C in six different solvents

Compd	λ^a	λ^b	λ^c	λ^d	λ^e	λ^f	$\Delta\lambda^g$
A	656	685	731	744	688	688	32
B	771	805	990	975	982	975	219
C	755	803	979	966	978	973	224

[a b c d e f] The maximum absorption wavelength (nm) of chromophores measured in dioxane, toluene, dichloromethane, chloroform, acetone, acetonitrile, respectively. [g] $\Delta\lambda=\lambda(max)-\lambda(min)$. $\lambda(max)$ and $\lambda(min)$: the maximum and minimum absorption wavelength of six solvents.

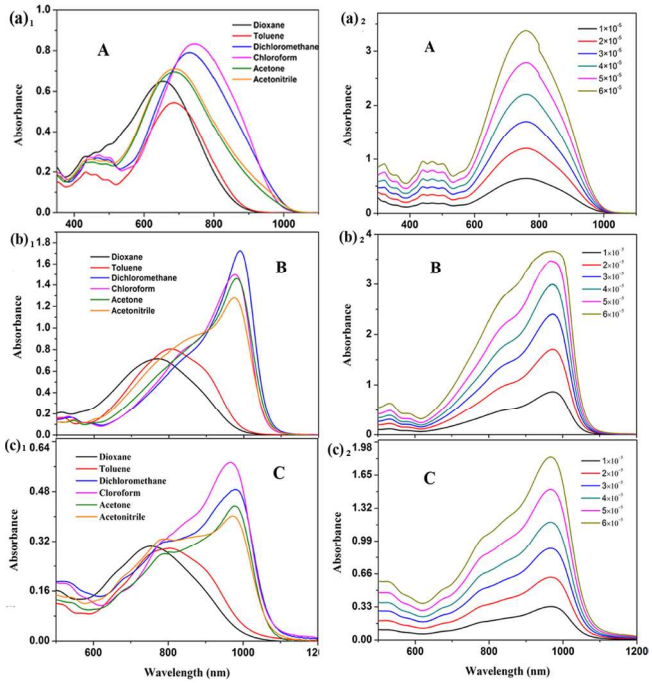

Fig. 1 UV-Vis-NIR spectra of chromophores **A, B** and **C** in six different solvents (left), UV-Vis-NIR spectra of chromophores **A**, **B** and **C** in $CHCl_3$ with six different concentrations (right).

UV-Vis Spectra Analysis. To reveal the dependence of the electronic absorption of chromophores **A**, **B** and **C** on their different donor and acceptor structures, the UV-Vis-NIR absorption spectra were investigated in six aprotic solvents (10^{-5} M) with different dielectric constants (Fig. 1, left). As Table 2 shown, a red-shift of the maximum absorption wavelengths (λ_{max}) from chromophore **A** to **B** or **C** was found due to the increased π-acceptor strength. For the weaker TCF acceptor-containing chromophore **A**, the λ_{max} exhibited a red-shift initially and then followed by a blue-shift with the increase of the dielectric constant from dioxane to acetonitrile along with the nearly identical spectral shape. This blue-shift phenomenon was called inverted solvatochromism, which was related to the μ change between the ground state (μ_g) and the excited state (μ_e) of chromophore molecule in different solvents. This meant that the μ_g was less than μ_e in non- to weakly polar solvents while it was larger than μ_e in highly polar solvents for chromophore **A**. In contrast, for the stronger CF_3-Ph-TCF acceptor-containing chromophores **B** and **C**, broad absorption bands were also observed in lower polar solvents. However, in more polar solvents from chloroform to acetonitrile, they could be both polarized close to the cyanine limit (the neutral and charge-separated limiting resonance forms contributed equally to the ground state) because of their similar stronger donor and acceptor pair. For the cyanine-like chromophores **B** and **C**, the most bathochromically shifted spectra usually exhibit two noticeable common features including the smallest fwhm (full width at half maximum) and the most intensified absorbance, demonstrating that chromophore with stronger acceptor had narrower energy gap and was easier to achieve charge distribution between the donor and acceptor parts. In addition, chromophores **B** and **C** both showed significant solvatochromic shift (219 and 224 nm, respectively) than that of chromophore **A** (32 nm) in solvents with different polarities (Table 2), which meant that chromophores **B** and **C** were more polarizable. Remarkably, λ_{max} of chromophores **B** and **C** was located in near

infrared region (near 1000 nm), indicating that these chromophores could have some potential applications in the field of infrared-absorbing dyes and pigments.[47]

The UV-Vis-NIR absorption spectra of three chromophores in chloroform with different concentrations were shown in Fig. 1 (right) for the study of the molecular aggregation. As the chromophore concentration increase, chromophores **A** and **B** showed larger extinction coefficients than chromophore **C**. It was speculated that chromophores with bulky TBDMS groups could be easily isolated from adjacent molecules. Therefore, they were easier to absorb photons for ICT. This indicated that the intensity of the absorption increased after the protection of the hydroxyl group of the donor. In all cases, additionally, the absorption band shapes and the λ_{max} were almost unchanged with increasing concentrations, suggesting that no strong ground state aggregation and crystallization behavior were appeared for chromophores **A**, **B** and **C**.

Table 3. Electrochemical properties of three chromophores

Compd	E_{ox} (V)	E_{red}[b] (V)	HOMO[a] (eV)	LUMO[b] (eV)	E_g[c] (eV)
A	0.35	-0.81	-4.79	-3.59	1.20
B	0.33	-0.59	-4.73	-3.81	0.92
C	0.33	-0.61	-4.73	-3.79	0.94

[a] HOMO=-[4.4+Eox]; [b] LUMO=-[4.4+Ered]; [c] E_g=-(HOMO-LUMO)

Electrochemical properties. Cyclic voltammetry (CV) measurement was usually used as an efficient method to determine the redox properties of chromophores. All three chromophores were tested in degassed acetonitrile solutions containing 0.1 M tetrabutylammonium hexafluorophosphate (TBAPF) as the supporting electrolyte. As shown in Table 3 and Fig. S1 (supporting information), the similar oxidative potentials of chromophores **A, B** and **C** were recorded at around 0.35, 0.33 and 0.33 V, respectively. In contrast, the reductive potentials were recorded at around -0.81, -0.59 and -0.61 V, respectively. The absolute values of the reductive potentials of chromophores **B** and **C** were smaller than that of chromophore **A** due to their increased acceptor strength.

Furthermore, the HOMO and LUMO levels of three chromophores were calculated from their corresponding oxidation and reduction potentials, respectively. The HOMO and LUMO levels showed the similar trend with respect to the redox potentials. And the energy gaps (E_g) of them were also calculated and shown in Table 3. The decreased energy gaps from chromophore **A** to chromophores **B** and **C** were in consistent to the UV-Vis-NIR spectra analysis.

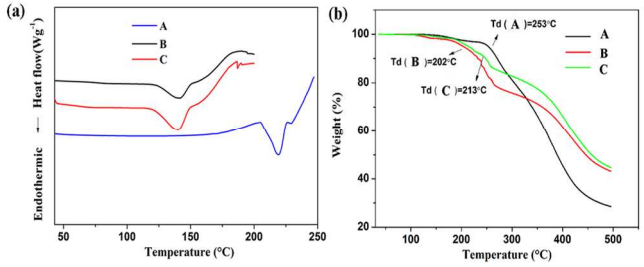

Fig. 2 The DSC (a) and TGA (b) curves of chromophores **A**, **B** and **C** with a heating rate of 10 °C /min in nitrogen.

Thermal Analysis. The thermal properties of chromophores **A**, **B** and **C** were evaluated by differential scanning calorimetry (DSC) and thermal gravimetric analysis (TGA) in nitrogen (Fig. 2 and Table 3). The degradation temperatures (T_d) of chromophores **A**, **B** and **C** for 5% weight loss were all higher than 200 °C. Chromophores **B** and **C** based on CF_3-Ph-TCF acceptor displayed the lower T_d than that of chromophore **A**, possibly owing to the instability of CF_3-Ph-TCF acceptor. In spite of this, the result temperatures were still sufficient for NLO devices. Moreover, these two chromophores appeared as amorphous solids with a glass transition temperature (T_g) at 142 and 140 °C, respectively. While chromophore **A** based on TCF acceptor showed a T_g at 218 °C, which was higher than chromophores **B** and **C**. The improved glass-forming ability of chromophores **B** and **C** were mainly attributed to the increased steric hindrance of the CF_3-Ph-TCF acceptor bearing benzene ring and trifluoromethyl substituents on the furan ring, which prevented close packing of chromophore molecules.[18]

Table 3 Thermal properties of chromophores **A, B** and **C**.

Compd	T_g/°C	T_d/°C
A	218	253
B	142	202
C	140	213

Table 4 Calculated theoretical parameters (dipole moment (μ)[a], total hyperpolarizability (β_{tot})[a], first-order polarizability (α)[a] and BLA)[b]

Compd	Sol	μ D	β_{tot} 10^{-30}esu	α a.u.	BLA Å
A	VC	24.38	978.7	831	-0.044
	DO	31.29	2240.2	1299.6	-0.035
	CF	36.75	3348.4	1547.0	-0.025
	DC	40.15	3978.6	1700.6	-0.019
	AC	43.11	4415.9	1817.5	-0.014
	AN	44.15	4429.6	1859.3	-0.012
B	VC	25.72	1180.1	946	-0.039
	DO	34.03	2349.6	1465.5	-0.024
	CF	41.84	2917.6	1759.6	-0.011
	DC	46.94	2515.4	1910.9	-0.003
	AC	51.17	1359.9	2000.2	0.004
	AN	52.65	1327.8	2022.1	0.007
C	VC	25.94	1208.4	905	-0.039
	DO	34.23	2478.9	1369.3	-0.024
	CF	41.99	3124.6	1655.2	-0.011
	DC	47.24	2739.3	1798.5	-0.003
	AC	51.64	1445.8	1878.1	0.004
	AN	53.20	1314.5	1899.6	0.007

[a]: VC: vacuum; DO: 1,4-dixoane; CF: chloroform; DC: dichloromethane; AC: acetone; AN: acetonitrile. [a] calculated at the CAM-B3LYP/6-31+G* level, [b] calculated at the B3LYP/6-31G level

DFT Calculations. DFT calculation was reported as an efficient method to deeply study the structure-property relationship of the molecules.[18, 19] Thus, to obtain the effect of the acceptor and slight donor modification dependent on ground-state polarization of this new series of julolidinyl-based chromophores, all chromophores (**A**, **B** and **C**) were optimized in vacuum and five different solvents at the B3LYP/6-31G level. In this study, the spin multiplicity of the ground states for chromophores A, B and C is 1, that is to say the ground states

are singlet states. The NLO properties of these three chromophores including μ, first-order polarizability (α), and the static total hyperpolarizability (β_{tot}) parameters were calculated at the CAM-B3LYP/6-31+G* level based on the B3LYP/6-31G optimized geometries, and were shown in Fig. 3 and displayed in Table 4. Besides, the electronic transition properties of these choromophores also were checked by the time-dependent (TD)-CAM-B3LYP/6-31+G* method. All the calculations were performed using Gaussian 09 program[33] in this study.

As is shown, the μ and α values of all chromophores displayed a similar increasing trend with the increase of the solvent polarity. Meanwhile, the μ and α values increased from chromophore **A** to chromophores **B** and **C** with the increased electron acceptor strength in all solvents. The β_{tot} values of three chromophores were distinctive. The β_{tot} value of chromophore **A** showed increasing trend with the increase of solvent polarity. By contrast, the β_{tot} values of chromophores **B** and **C** with strong acceptor increased initially in weak polar solvents and reached to the maximum in chloroform, then decreased in high-polar solvents such as acetone and acetonitrile. Specially, the β_{tot} value of chromophore **B** was smaller than that of chromophore **C** in solvents such as dioxane, chloroform, dichloromethane and acetone. This phenomenon may be caused by the strong interaction between the hydroxy of chromophore **C** and the solvents.

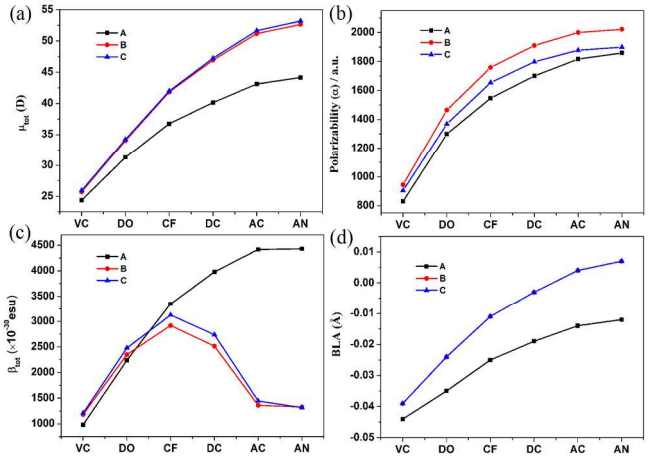

Fig. 3 The solvent dependence of (a) μ_{tot}, (b) α, (c) β_{tot}, (d) BLA were calculated in gas phase and five solvents. For (d), the red line and the blue line overlapped. VC: vacuum; DO: 1,4-dixoane; CF: chloroform; DC: dichloromethane; AC: acetone; AN: acetonitrile.

By tuning the appropriate molecule structure to regulate the relative ratio of two limiting resonance forms (neutral and zwitterionic form) in ground state, it can optimize the optical nonlinearities.[34] The positive and negative property of BLA indicated that, in relative low polar solvents, for chromophores **B** and **C**, the neutral form prevailed in the ground state. Whereas in high polar solvents, the zwitterionic form prevailed, meaning that chromophores **B** and **C** were more polarizable than chromophore **A**. It was in good accordance with the photophysical analysis. On the other hand, for push-pull polyene chromophores, the β value can be related with the ground state polarization as well as BLA.[32] As shown in Fig. 3, the BLA values of chromophores **B** and **C** were closer to zero with respect to chromophore **A**, owning to their cyanine-like electronic structures which was corroborated by UV-Vis-NIR spectral results. The BLA value for chromophore **A** was more close to $\pm$ 0.05 $\pm$ 0.01 Å with respect to chromophores **B** and **C**, which demonstrated the relative relationship between the β and the BLA reported before.[32] In addition, chromophores **B** and **C** displayed almost the same BLA according to the similar main CT structure. Thus, chromophore with stronger donor and acceptor doesn't possess the larger β value. Reasonable options and designs are important for chromophores with large EO properties.

Finally, the frontier molecular orbitals of chromophores **A**, **B** and **C** were calculated in vacuum and sketched in Fig. 4. In the ground state, all three chromophores displayed nearly coplanar configuration, resulting the better π-delocalization. It could also be seen from electron density distributions of the highest occupied molecular orbital (HOMO) and the lowest unoccupied molecular orbital (LUMO). The HOMO in three chromophores was of π nature and mainly localized on the julolidinyl-based donor and conjugated bridge, while the LUMO was mainly localized in TCF or CF_3-Ph-TCF group and the conjugated bridge, especially in the acceptor. Furthermore, the LUMO in chromophores **B** and **C** was more concentrated on the acceptor part than that in chromophore **A**. Then, TD-CAM-B3LYP/6-31+G*) calculations demonstrated the ICT character of the HOMO→LUMO transition. The topology of the the frontier molecular orbitals demonstrated the ICT character of the HOMO→LUMO transition.[48] It also displayed that the energy gap (E_g) between HOMO and LUMO of chromophore **A** (1.87 eV) was larger than that of chromophores **B** and **C** (1.77 and 1.81 eV). Thus, the ICT for chromophores **B** and **C** was easier than that to TCF acceptor for chromophore **A**. The present calculated results were in good consist with the spectral analysis mentioned above.

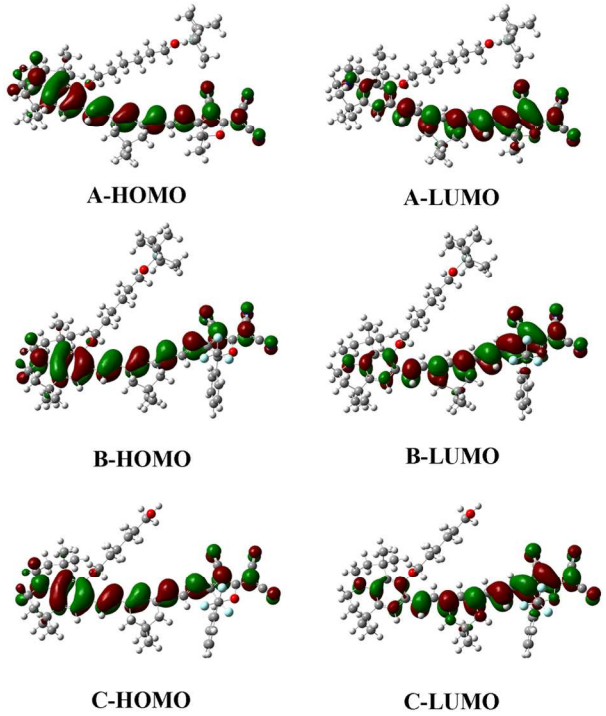

Fig. 4 The frontier molecular orbitals of chromophores **A, B** and **C**.

Electro-optic Coefficient Measurements. To evaluate the NLO activity of the chromophores **A**, **B** and **C**, their poled thin films were prepared. After conserving at ambient environment for a month, three chromophores were tested by TLC. It

showed that chromophores **A** and **C** were chemically stable but chromophore **B** turned to the new yellowish-brown compound and chromophore **C** without protected groups. It was speculated that chromophore **B** with strong donor and acceptor was related to the stronger ICT ability than chromophore **A**, which made it more sensitive to the ambient environment and thus lead to the relatively poor photostability and chemical stability. Thus, we tested the electro-optic coefficient of chromophores **A** and **C**. Finally, chromophores **A** was doped in **APC** with the content 20 wt% as the typical guest-host polymer. In addition, the large μ, the narrow E_g and without the protection of TBDMS groups resulted in poor compatibility of chromophore **C** in **APC**. Thus, low content (10 wt%) of chromophore **C** was doped in **APC** film for EO measurement.

Therefore, through changing the poling temperature, poling voltage and poling time, the optimum poling condition were obtained. The guest-host polymers **A/APC** (T_g =138 °C) and **C/APC** (Tg =147 °C) were both poled at each optimum poling condition. The optimized poling temperature was always 5 °C higher than T_g of the EO film, and the poling voltage was in the range of 1.1~1.2 kV. By doping chromophore **A** in to **APC** with a loading of 20 wt%, the large r_{33} value of up to 192 pm/V at 1.31 μm can be achieved. It exhibited a nearly seven times improvement over the value for EO polymers doped with chromophore **C** (24 pm/V), and clearly indicated the good potential of these materials for EO applications. In contrast, chromophore **C** displayed the similar r_{33} to the ever reported julolidinyl-based chromophore **3** (20 pm/V at 1.31 μm) with the same conjugated bridge and acceptor[18], which demonstrated that the acceptor here had more effect on EO properties than the branch. Such a subtle difference in the structure of the acceptor between CF_3-Ph-TCF and TCF could change the EO property of chromophores in a large degree. Chromophores with stronger CF_3-Ph-TCF acceptor were reported showing larger NLO properties than chromophores with normal TCF acceptor.[14] However, in this study, relatively weak TCF acceptor could profoundly improve the micro- and macro-scopic nonlinearities for chromophore **A** with julolidinyl-based donor and CLD-type bridge.

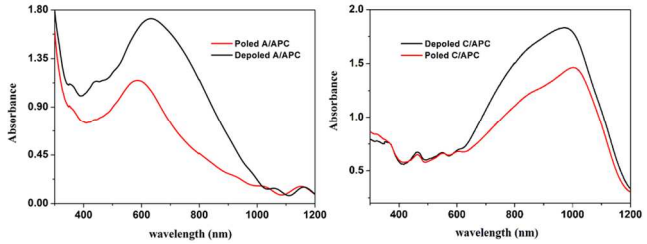

Fig. 5 Absorption spectra of depoled and poled films of chromophores **A** and **C** in **APC**.

To get a deep understanding of the electronic poling mechanism for chromophores **A** and **C**, the absorption spectra of depoled and poled films were recorded. As shown in Fig. 5, significant changes in the intensity and the shape of the ICT absorption spectra were induced by electronic poling. The order parameter $\Phi = 1\text{-}A/A_0$ was described as the criterion for the degree of polarization, where the A and A_0 are the absorbance of poled and depoled EO polymer films. Based on the above poling conditions, the poled films of **A/APC** gave larger Φ values than that of **C/APC**. It demonstrated that chromophore **A** showed larger poling efficiency with respect to chromophore **C**. This might be attributed to the large protected TBDMS group that decrease the interaction of chromophore molecules. Moreover, the recorded high conductivity of chromophore **C** under the poling conditions could also resulted in the decreased β value and the poor poling efficiency,[18] which also lead to its poor r_{33} value. Above all, this julolidinyl-based polyene chromophores represent a new kind of push-pull framework that could be useful for new generation NLO materials and devices.

Experimental

Materials and Instrumentation. Microwave irradiation reactions were carried out in a MCR-3 microwave reactor. Reactions were performed in open glass vessels (capacity 50 mL). All reagents were purchased from commercial sources and were used as received unless otherwise specified. Solvents such as DMF, THF, EtOH, toluene and diethyl ether were freshly treated and distilled prior to use according to the common purification procedures; the dielectric constants of six different solvents are 1,4-dixoane: 2.25, toluene: 2.38, chloroform: 4.81, dichloromethane: 8.93, acetone: 20.7, acetonitrile: 37.5, respectively. The electron donor, the electron bridge and the TCF or CF_3-Ph-TCF acceptors were prepared before.[14, 45] ^{1}H NMR and ^{13}C NMR spectra were measured on an AVANCE 400 (Bruker) spectrometer (400 MHz) using tetramethylsilane (TMS; δ = 0 ppm) as the internal standard. UV-Vis-NIR spectra were obtained using a HITACHI U-2001 spectrometer. The Thermo gravimetric analysis (TGA) curves were recorded with a TA-instrument Q50 analyzer at a heating rate of 10 °C /min in nitrogen at a flow rate of 50 cm^3/min. Differential scanning calorimetry (DSC) measurements were performed on a TA5000, 2910MDSC with a heating rate of 10 °C /min under the protection of nitrogen. The thickness of the films were measured with an Ambios Technology XP-1 profilometer. The MS spectra were obtained on MALDI-TOF (Matrix Assisted Laser Desorption/Ionization of Flight) on BIFLEXIII (Broker Inc.) spectrometer. The DFT quantum chemical methods using Gaussian 09 software package were carried out.

Preparation of Compound 3. Under N_2 atmosphere to a solution of compound 1 (8-hydroxy-1,1,7,7-tetramethyl-formyljulolidine, 2.73 g, 0.01 mol) in anhydrous DMF was added 6-chlorohexan-1-ol (2.05 g, 0.015 mol) and K_2CO_3 (2.08 g, 0.015 mol). The mixture was irradiated under microwaves (140 °C) for 40 min and then poured into water until it was cooled to the ambient temperature. The resulting solutions were filtered and then extracted with ethyl acetate. The combined organic extracts were washed with brine and then dried over $MgSO_4$ and filtered. After the removal of the solvent, the residue was purified by column chromatography using hexane and acetone as eluent to give the product yellow solids (3.73 g, yield: 82%). MS (MALDI-TOF), m/z: 373.19 $[M+H]^+$; ^{1}H NMR (400 MHz, $CDCl_3$, ppm) δ 9.92 (s, 1H), 7.57 (s, 1H), 3.96 (t, 2H), 3.66 (t, 2H), 3.29 (t, J = 5.9 Hz, 2H), 3.25 – 3.20 (m, 2H), 2.02 (s, 1H), 1.89 (m, 2H), 1.76 – 1.66 (t, 4H), 1.61 (d, J = 6.6 Hz, 2H), 1.55 – 1.44 (m, 4H), 1.42 (s, 6H), 1.26 (s, 6H). ^{13}C NMR (101 MHz, $CDCl_3$, ppm) δ 187.83 , 162.08 , 148.38 , 126.09 , 125.52 , 120.73 , 117.03 , 78.60 , 62.44 , 47.46 , 46.81 , 39.34 , 35.62 , 32.63 , 32.43 , 32.02 , 30.22 , 30.00 , 29.73 , 25.76.

Preparation of Compound 5. A mixture of compound 3 (3.37 g, 0.01 mol), compound 4 (isophorone, 1.66 g, 0.012 mol), sodium ethoxide (0.013 mol, 0.3 g sodium dissolved in 2 mL anhydrous ethanol) in 10 mL anhydrous ethanol was irradiated

under microwaves (120 °C) for 30 min. Then the reaction finished and cooled to the room temperature. After the solvent was evaporated, the residue was purified by column chromatography use hexane/ethyl acetate as eluent to give the product as dark red solids (4.78 g, yield: 97%). MS (MALDI-TOF), m/z: 493.36 $[M+H]^+$; ^{1}H NMR (400 MHz, $CDCl_3$, ppm) δ 7.20 (s, 1H), 7.11 (d, *J* = 16.1 Hz, 1H), 6.60 (d, *J* = 16.1 Hz,1H), 5.96 (s, 1H), 3.72 (t, *J* = 6.7 Hz, 2H), 3.59 (t, *J* = 6.5 Hz, 2H), 3.13 (t, 2H), 3.06 (t, 2H), 2.40 (s, 2H), 2.22 (s, 2H), 2.09 (s, 2H), 1.86 – 1.75 (m, 3H), 1.65 (t, 4H), 1.57 (dd, *J* = 14.2, 7.0 Hz, 2H), 1.52 – 1.44 (m, 2H), 1.45 – 1.37 (m, 2H), 1.34 (s, 6H), 1.21 (s, 6H), 1.02 (s, 6H). ^{13}C NMR (101 MHz, $CDCl_3$, ppm) δ 199.20 , 156.12 , 155.92 , 143.17 , 131.54 , 131.54 , 125.67 , 123.19 , 122.76 , 121.96 , 121.14 , 115.61 , 74.46 , 61.55 , 50.32 , 46.33 , 45.81 , 39.03 , 38.44 , 35.44 , 35.44 , 32.26 , 31.68 , 31.22 , 30.05 , 29.19 , 27.58 , 25.26 , 24.95.

Preparation of Compound 6. A mixture of compound 5 (4.94 g, 0.01 mol), tert-butyldimethylsilyl chloride (2.26 g, 0.015 mol) and imidazole (1.70 g, 0.025 mol) were dissolved in 40 mL anhydrous dimethylformamide. After stirring at room temperature overnight, the reaction mixture was poured into water and extracted with ethyl acetate. The combined organic extracts were washed with brine and then dried over $MgSO_4$ and filtered. After the solvent was evaporated, the residue was purified by column chromatography use hexane/ethyl acetate as eluent to give the product as orange solids (4.86 g, yield: 80%). MS (MALDI-TOF), m/z: 607.98 $[M+H]^+$; ^{1}H NMR (400 MHz, $CDCl_3$, ppm) δ 7.24 (s, 1H), 7.14 (d, *J* = 16.1 Hz, 1H), 6.63 (d, *J* = 16.2 Hz, 1H), 5.97 (s, 1H), 3.75 (t, *J* = 6.4 Hz, 2H), 3.58 (t, *J* = 6.3 Hz, 2H), 3.15 (t, 2H), 3.07 (t, 2H), 2.43 (s, 2H), 2.25 (s, 2H), 1.88 – 1.76 (m, 2H), 1.68 (t, 4H), 1.58 – 1.44 (m, 5H), 1.44 – 1.40 (m, 2H), 1.37 (s, 6H), 1.24 (s, 6H), 1.05 (s, 6H), 0.84 (s, 15H). ^{13}C NMR (101 MHz, $CDCl_3$, ppm) δ 199.84 , 157.13 , 156.47 , 132.34 , 124.56 , 123.88 , 122.84 , 75.59 , 63.09 , 51.41 , 47.39 , 46.87 , 40.06 , 39.33 , 36.48 , 33.25 , 32.87 , 32.68 , 32.25 , 31.12, 30.21 , 28.63 , 26.32 , 26.00 , 18.35 , -5.23.

Preparation of Compound 7. Under N_2 atmosphere to the mixture of NaH (0.19 g, 0.00774 mol) in dry THF was added diethyl cyano-phosphonate (1.37 g, 0.00774 mol) dropwise by syringe at 0 °C with an ice bath. After the solution became clear, compound 5 (2.34 g, 0.00386 mol) in dry THF was added. The mixture was refluxed for 3 h and then poured into a saturated solution of ammonium chloride and extracted with ethyl acetate; the combined organic extracts were washed with brine and dried over $MgSO_4$ and then filtered. After removal of the solvent, the residue was purified by column chromatography using hexane/ethyl acetate as eluent to give the product as orange oil (1.95 g, yield: 80%). The ratio of the Z : E isomers is 42:58 calculated by the integration of respective protons in ^{1}H NMR. MS (MALDI-TOF), m/z: 631.02 $[M+H]^+$; ^{1}H NMR (400 MHz, $CDCl_3$, ppm) δ 7.25 (s, 1H), 6.67 (d, *J* = 19.3 Hz, 1H), 6.57 (d, *J* = 16.1 Hz, 1H), 6.18 (s, 1H), 4.99 (s, 1H), 4.81 (s, 1H), 3.86 (t, *J* = 6.4 Hz, 1H), 3.74 (dd, *J* = 10.1, 6.4 Hz, 2H), 3.57 (dd, *J* = 11.3, 6.3 Hz, 3H), 3.15 – 3.09 (m, 2H), 3.08 – 3.03 (m, 2H), 3.03 – 2.97 (m, 1H), 2.96 – 2.92 (m, 1H), 2.42 (s, 1H), 2.27 (s, 2H), 2.17 (s, 1H), 1.36 (s, 14H), 1.23 (m, 11H), 1.27 – 1.18 (m, 11H), 0.96 (d, *J* = 13.8 Hz, 7H), 0.85 (s, 16H). ^{13}C NMR (101 MHz, $CDCl_3$) δ 157.31 , 156.96 , 155.53 , 145.33 , 144.91 , 142.48 , 127.98 , 125.67 , 125.52 , 124.01 , 123.75 , 123.37 , 121.48 , 121.33 , 121.21 , 121.11 , 117.66 , 116.95 , 116.33 , 90.41 , 88.94 , 74.10 , 62.02 , 46.31 , 45.82 , 43.63 , 41.07 , 39.19 , 38.08 , 35.62 , 31.83 , 31.63 , 31.20 , 30.23 , 29.98 , 29.26 , 27.21 , 25.26 , 24.96 , 17.29 , -6.27.

Preparation of Compound 8. The solution of compound 7 (1.89 g, 0.003 mol) in 20 mL of dry toluene was cooled to -78 °C and the solution of DIBAL in hexane (1.0 M, 6 mL, 0.006 mol) was added dropwise. After being kept at -78℃ for 2 hours, wet silica gel (1.5 g) with 5.0 mL of water was added and the reaction mixture was stirred at 0 °C for 1 hour and then stirred at room temperature for 1 hour. After filtered and washed with ethyl acetate, the mixture was removed most of low boiling point solvent, and the residue mixture was purified by column chromatography using hexane/ethyl acetate as eluent to give the product as dark red solids (1.34 g, yield: 70%). The ratio of the Z : E isomers is 27:73% calculated by the integration of respective protons. MS (MALDI-TOF), m/z: 633.02 $[M+H]^+$; ^{1}H NMR (400 MHz, $CDCl_3$, ppm) δ 10.16 (d, *J* = 7.9 Hz, 0.3H), 9.99 (d, *J* = 8.2 Hz, 0.7H), 7.20 (d, *J* = 17.4 Hz, 1H), 6.95 (dd, *J* = 16.0, 9.3 Hz, 1H), 6.66 (t, *J* = 14.7 Hz, 1H), 6.24 (s, 1H), 5.85 (d, *J* = 8.0 Hz,0.7 H), 5.64 (d, *J* = 7.8 Hz, 0.3H), 3.75 (t, 2H), 3.58 (t,29H), 3.12 (t, 2H), 3.05 (t, 2H), 2.64 (s, 1H), 2.32 (s, 2H), 2.23 (s, 1H), 1.88 – 1.75 (m, 4H), 1.67 (t, 4H), 1.59 – 1.45 (m, 2H), 1.40 (dd, *J* = 10.9, 2.2 Hz, 2H), 1.36 (s, 6H), 1.23 (s, 6H), 1.01 (s, 6H), 0.85 (s, 9H). ^{13}C NMR (101 MHz, $CDCl_3$, ppm) δ 190.24 , 189.35 , 156.91 , 156.65 , 147.22 , 143.56 , 129.15 , 127.34 , 126.61 , 125.81 , 125.12 , 122.51 , 122.18 , 117.36 , 75.20 , 63.05 , 47.34 , 46.84 , 40.20 , 39.40 , 38.89 , 36.66 , 32.86 , 32.66 , 32.23 , 31.27 , 31.03 , 30.28 , 28.45 , 26.29 , 25.99 , 18.31 , -5.24.

Preparation of Chromophore A. A mixture of compound 5 (1.90 g, 0.003 mol) and 2-dicyanomethylen-3-cyano-4,5,5-trimethyl-2,5-dihydrofuran (TCF) (0.90 g, 0.0045 mol) in 10 mL of ethanol was irradiated under microwaves (120 °C) for 15 min. The resulting mixture was removed the solvent and purified through column chromatography using hexane/ethyl acetate as eluent to give the product as dark solids (1.82 g, yield: 75%). The ratio of the Z : E isomers is 20:80% calculated by the integration of respective protons. MS (MALDI-TOF), m/z: 814.02 $[M+H]^+$; ^{1}H NMR (400 MHz, $CDCl_3$) δ 8.00 (t, J = 13.5 Hz, 1H), 7.32 (s, 1H), 7.10 (d, J = 15.9 Hz, 1H), 6.76 (d, J = 16.7 Hz, 1H), 6.40 (s, 1H), 6.33 (d, J = 11.9 Hz, 1H), 6.24 (d, J = 15.0 Hz, 1H), 3.80 (t, 2H), 3.63 (t, 2H), 3.21 (d, J = 27.8 Hz, 4H), 2.43 (d, J = 6.4 Hz, 4H), 1.86 (dd, J = 14.2, 6.7 Hz, 2H), 1.71 (s, 4H), 1.68 (s, 6H), 1.54 (s, 4H), 1.42 (s, 6H), 1.28 (d, J = 19.2 Hz, 12H), 1.05 (s, 6H), 0.89 (s, 12H). ^{13}C NMR (101 MHz, $CDCl_3$) δ 176.45 , 173.01 , 157.53 , 155.89 , 150.21 , 144.16 , 129.29 , 127.51 , 122.91 , 114.86 , 112.98 , 112.30 , 112.09 , 96.64 , 75.90 , 63.25 , 47.69 , 47.16 , 39.94, 36.48 , 32.93 , 32.41 , 31.57 , 31.04 , 30.44 , 30.20 , 28.64 , 26.71 , 26.46 , 26.16 , 18.49 , -5.12. $C_{51}H_{70}N_4O_3Si$: C, 75.13; H, 8.66; N, 6.86; O, 5.89; Si, 3.46.

Preparation of Chromophore B. The procedure for chromophore **A** was followed to prepare chromophore B from compound **8** as dark solids. MS (MALDI-TOF), m/z: 931 $[M+H]^+$; ^{1}H NMR (400 MHz, $CDCl_3$) δ 7.70 (t, 1H), 7.50 (s, 5H), 7.35 (s, 1H), 7.27 (d, J = 15.4 Hz, 1H), 6.78 (d, J = 15.6 Hz, 1H), 6.45 (s, 1H), 6.24 (d, J = 13.4 Hz, 1H), 3.68 – 3.55 (m, 4H), 3.31 (t, 2H), 3.23 (t, 2H), 2.43 (s, 2H), 1.93 – 1.81 (m, 2H), 1.78 – 1.65 (m, 2H), 1.55 (s, 4H), 1.47 – 1.46 (m, 2H), 1.45 (s, 1H), 1.43 (s, 1H), 1.41 (s, 6H), 1.29 (s, 2H), 1.25 (s, 2H), 1.01 (s, 6H), 0.96 (t, J = 7.4 Hz, 6H), 0.89 (s, 15H). ^{13}C NMR (101

MHz, $CDCl_3$) δ 166.69 , 131.32 , 129.89 , 128.42 , 127.82 , 126.50 , 125.71 , 123.75 , 122.26 , 113.43 , 64.54 , 62.06 , 46.36, 38.68, 34.83 , 31.84 , 31.60 , 31.19 , 30.68 , 29.56 , 29.45 , 29.28 , 28.80 , 28.68 , 27.52 , 27.14 , 25.31 , 24.96 , 24.57, 18.17 , 17.35 , 12.71 , -6.28. $C_{56}H_{69}F_3N_4O_3Si$: C, 72.24; H, 7.46; F, 6.12; N, 6.03; O, 5.14; Si, 3.01.

Preparation of Chromophore C. The procedure for chromophore **A** was followed to prepare chromophore **C** from compound **8** as dark solids. MS (MALDI-TOF), m/z: 817.02 (M^+); ^{1}H NMR (400 MHz, $CDCl_3$) δ 8.07 (t, 1H), 7.50 (s, 5H), 7.35 (s, 1H), 7.29 (d, J = 15.8, 1H), 6.79 (d, J = 14.9 Hz, 1H), 6.47 (s, 1H), 6.23 (d, J = 14.3 Hz, 1H), 3.80 (s, 2H), 3.66 (s, 2H), 3.47 (s, 1H), 3.32 (t, 2H), 3.25 (t, 2H), 2.37 – 2.24 (m, 2H), 1.87 (m, 2H), 1.81 – 1.68 (m, 4H), 1.69 – 1.59 (m, 2H), 1.57 – 1.53 (m, 2H), 1.53 – 1.44 (m, 2H), 1.41 (s, 6H), 1.29 (s, 6H), 0.99 (d, J = 18.1 Hz, 6H). ^{13}C NMR (101 MHz, $CDCl_3$) δ 177.08 , 159.59 , 146.78 , 135.98 , 131.87 , 130.34 , 128.52 , 127.65 , 125.63 , 124.39 , 123.44 , 115.22 , 113.43 , 112.90 , 63.65 , 48.32 , 40.62 , 36.69 , 33.56 , 33.10 , 32.66 , 31.22 , 30.69 , 29.27, 27.02. $C_{50}H_{55}F_3N_4O_3$: C, 73.50; H, 6.78; F, 6.99; N, 6.87; O, 5.86.

Preparation of EO polymer thin films. Because the chromophore **B** tended to be chemically unstable, chromophores **A** and **C** were doped in **APC** with the content of 20 wt% and 10 wt%, respectively. The resulting solutions of these polymers were filtered through 0.2 μm PTFE-syringe filters and spin-coated onto the indium tin oxide (ITO) glass substrates. Then, the EO polymer films were dried overnight under vacuum. The thickness of the yielding optical quality thin films was 1.5-2.5 μm. The ITO substrates were selected with suitable conductivity, low reflectivity and good transparency. They were cleaned by isopropanol, acetone and ethanol sequentially in an ultrasonic bath before use to minimize the contribution from multiple reflections in EO measurements.[36]

NLO Measurement of Poled Films. The films of **A/APC** (with 20 wt%) and **C/APC** (with 10 wt%) were dried completely and then poled at around 143 °C and 152 °C for about 25 min following the typical corona poling protocols, respectively. The poled samples were then cooled down rapidly to the ambient temperature, and the applied field was removed. After that, a thin layer of aluminium (50~100 nm) was then sputtered on the top of the poled polymer films as the top electrode and mirror. The r_{33} values of poled films were measured by the Teng-Man Simple Reflection method at the wavelength of 1.31 μm using a carefully selected thin ITO electrode.

Conclusions

A facile MAOS method have been introduced to synthesize a series of highly hyperpolarizable julolidinyl-based CLD-type chromophores with TCF or CF_3-Ph-TCF acceptors in almost two times large overall yields of usual. This new method was available to synthesize the CLD-type chromophores, and could afford the enhanced reaction rates as well as high yields of pure products. Moreover, the different strength of the acceptors in these chromophores can provide an efficient way to effectively tune the ground state polarization and the ICT. All three chromophores showed adequate thermal stability according to the thermal analysis. The μ, α, β and BLA of chromophores were calculated in gas and liquid phase to study the solvent dependence properties of these parameters. Guest-host EO film **A/APC** with a loading density of 20 wt% chromophore **A** with TCF acceptor exhibited a large r_{33} value of 192 pm/V at 1.31 μm. It showed seven times higher than EO film **C/APC** doping chromophore **C** with CF_3-Ph-TCF acceptor. In our work, chromophore **A** with relatively weak TCF acceptor profoundly improved the micro- and macro-scopic EO activity of materials. Consequently, this series of chromophores with high EO performance, especially chromophore **A**, can be used for the development of novel dielectric photonic and NLO devices.

Acknowledgements

We are grateful to the National Natural Science Foundation of China (Nos. 11104284, 21003143 and 61101054) for financial support. All calculations were performed on the cluster of Key Laboratory of Theoretical and Computational Photochemistry, Ministry of Education, China.

Notes and references

[a] Key Laboratory of Photochemical Conversion and Optoelectronic Materials, Technique Institute of Physics and Chemistry, Chinese Academy of Sciences, Beijing, 100190, PR China
[b] University of Chinese Academy of Sciences, Beijing 100049, PR China

† Electronic supplementary information (ESI) available: Quantum chemical calculations, ^{1}H and ^{13}C NMR spectra of compounds. See DOI: 10.1039/b000000x/

1 J. Luo, X.-H. Zhou and A. K. Y. Jen, *J. Mater. Chem.*, 2009, **19**, 7410-7424.
2 L. R. Dalton, P. A. Sullivan, D. H. Bale and B. C. Olbricht, *Solid State Electron*, 2007, **51**, 1263-1277.
3 L. R. Dalton, W. Steier and B. Robinson, *J. Mater. Chem.*, 1999, **9**, 1905-1920.
4 D. H. Park, C. H. Lee and W. N. Herman, *Opt Express*, 2006, **14**, 8866-8884.
5 Y. Enami, C. Derose, D. Mathine, C. Loychik, C. Greenlee, R. Norwood, T. Kim, J. Luo, Y. Tian and A.-Y. Jen, *Nature Photonics*, 2007, **1**, 180-185.
6 C. Z. a. L. R. Dalton, *Chem. Mater.*, 2001, **13**, 3043-3050.
7 X. Zhang, A. Hosseini, J. Luo, A. K. Y. Jen and R. T. Chen, 2014, pp. 89910O-89910O-89916.
8 L. R. Dalton, in Polymers for Photonics Applications I, ed. K.-S. Lee, Springer Berlin Heidelberg, 2002, pp. 1-86.
9 H. Xiao, H. Yin and X. Zhang, *Org. Lett.*, 2012, 14, 5282-5285.
10 W. C. W. Leu and C. S. Hartley, *Org. Lett.*, 2013, **15**, 3762-3765.
11 S.-i. Kato and F. Diederich, *Chem. Commun.*, 2010, **46**, 1994-2006.
12 W. Lin, Y. Cui, J. Gao, J. Yu, T. Liang and G. Qian, *J. Mater. Chem.*, 2012, **22**, 9202-9208.
13 A. Wojciechowski, M. M. Raposo, M. C. Castro, W. Kuznik, I. Fuks-Janczarek, M. Pokladko-Kowar and F. Bureš, *J. Mater. Sci: Mater. Electron*, 2014, **25**, 1745-1750.
14 Y. Liao, B. E. Eichinger, K. A. Firestone, M. Haller, J. Luo, W. Kaminsky, J. B. Benedict, P. J. Reid, A. K. Jen and L. R. Dalton, *J. Am. Chem. Soc.*, 2005, **127**, 2758-2766.
15 Z. Shi, J. Luo, S. Huang, X.-H. Zhou, T.-D. Kim, Y.-J. Cheng, B. M. Polishak, T. R. Younkin, B. A. Block and A. K.-Y. Jen, *Chem. Mater.*, 2008, **20**, 6372-6377.
16 Y. Liao, S. Bhattacharjee, K. A. Firestone, B. E. Eichinger, R. Paranji, C. A. Anderson, B. H. Robinson, P. J. Reid and L. R. Dalton, *J. Am. Chem. Soc.*, 2006, **128**, 6847-6853.

17 A. R. Morales, A. Frazer, A. W. Woodward, H.-Y. Ahn-White, A. Fonari, P. Tongwa, T. Timofeeva and K. D. Belfield, *J. Org. Chem.*, 2013, **78**, 1014-1025.
18 X.-H. Zhou, J. Luo, J. A. Davies, S. Huang and A. K. Y. Jen, *J. Mater. Chem.*, 2012, **22**, 16390-16398.
19 X.-H. Zhou, J. Davies, S. Huang, J. Luo, Z. Shi, B. Polishak, Y.-J. Cheng, T.-D. Kim, L. Johnson and A. Jen, *J. Mater. Chem.*, 2011, 21, 4437-4444.
20 J. L. Yen-Ju Cheng, Su Huang, Xinghua Zhou, Zhengwei Shi, Tea-Dong Kim,Denise H. Bale, Satsuki Takahashi, Andrew Yick, Brent M. Polishak, Sei-Hum Jang, Larry R. Dalton, Philip J. Reid, William H. Steier, and Alex K.-Y. Jen, *Chem. Mater.*, 2008, **20**, 5047-5054.
21 Z. Shi, J. Luo, S. Huang, B. M. Polishak, X.-H. Zhou, S. Liff, T. R. Younkin, B. A. Block and A. K. Y. Jen, *J. Mater. Chem.*, 2012, **22**, 951-959.
22 B. M. Polishak, S. Huang, J. Luo, Z. Shi, X.-H. Zhou, A. Hsu and A. K. Y. Jen, *Macromolecules*, 2011, **44**, 1261-1265.
23 J. D. Luo, Y. J. Cheng, T. D. Kim, S. Hau, S. H. Jang, Z. W. Shi, X. H. Zhou and A. K. Y. Jen, *Org. Lett.*, 2006, 8, 1387-1390.
24 T.-D. Kim, Z. Shi, J. Luo, S.-H. Jang, Y.-J. Cheng, X. Zhou, S. Huang, L. R. Dalton, W. Herman and A. K. Y. Jen, 2007, pp. 64700D-64700D-64714.
25 T.-D. Kim, J. Luo, Y.-J. Cheng, Z. Shi, S. Hau, S.-H. Jang, X.-H. Zhou, Y. Tian, B. Polishak, S. Huang, H. Ma, L. R. Dalton and A. K. Y. Jen, *J. Phys. Chem. C*, 2008, **112**, 8091-8098.
26 X.-H. Zhou, J. Luo, S. Huang, T.-D. Kim, Z. Shi, Y.-J. Cheng, S.-H. Jang, D. B. Knorr, R. M. Overney and A. K. Y. Jen, *Adv. Mater.*, 2009, 21, 1976-1981.
27 Z. Shi, W. Liang, J. Luo, S. Huang, B. M. Polishak, X. Li, T. R. Younkin, B. A. Block and A. K.-Y. Jen, *Chem. Mater.*, 2010, **22**, 5601-5608.
28 Y. V. Pereverzev, K. N. Gunnerson, O. V. Prezhdo, P. A. Sullivan, Y. Liao, B. C. Olbricht, A. J. P. Akelaitis, A. K. Y. Jen and L. R. Dalton, *J. Phys. Chem. C*, 2008, **112**, 4355-4363.
29 A. S. R. Cheng Zhang, Fang Wang, Jingsong Zhu, and Larry R. Dalton, *Chem. Mater.*, 1999, **11**, 1966-1968.
30 Y.-J. Cheng, J. Luo, S. Huang, X. Zhou, Z. Shi, T.-D. Kim, D. H. Bale, S. Takahashi, A. Yick, B. M. Polishak, S.-H. Jang, L. R. Dalton, P. J. Reid, W. H. Steier and A. K. Y. Jen, *Chem. Mater.*, 2008, **20**, 5047-5054.
31 J. Luo, S. Huang, Y.-J. Cheng, T.-D. Kim, Z. Shi, X.-H. Zhou and A. K. Y. Jen, *Org. Lett.*, 2007, **9**, 4471-4474.
32 M. Blanchard-Desce, V. Alain, P. V. Bedworth, S. R. Marder, A. Fort, C. Runser, M. Barzoukas, S. Lebus and R. Wortmann, *Chem.—Eur. J.*, 1997, **3**, 1091-1104.
33 J. V. Lockard, A. Butler Ricks, D. T. Co and M. R. Wasielewski, *J.Phys.Chem.Letter*, 2009, **1**, 215-218.
34 G. Wu, F. Kong, J. Li, W. Chen, C. Zhang, Q. Chen, X. Zhang and S. Dai, *Synthetic Metals*, 2013, **180**, 9-15.
35 G. Wu, F. Kong, J. Li, X. Fang, Y. Li, S. Dai, Q. Chen and X. Zhang, *J Power Sources*, 2013, **243**, 131-137.
36 J. Wu, C. Peng, H. Xiao, S. Bo, L. Qiu, Z. Zhen and X. Liu, *Dyes Pigm*, 2014, **104**, 15-23.
37 J. Wu, S. Bo, J. Liu, T. Zhou, H. Xiao, L. Qiu, Z. Zhen and X. Liu, *Chem. Commun.*, 2012, **48**, 9637-9639.
38 R. N. Gedye, F. E. Smith and K. C. Westaway, *Can. J. Chem.*, 1988, **66**, 17-26.
39 R. S. Varma, *Green Chem*, 1999, **1**, 43-55.
40 V. Polshettiwar and R. S. Varma, *Accounts of Chemical Research*, 2008, **41**, 629-639.
41 P. Lidström, J. Tierney, B. Wathey and J. Westman, *Tetrahedron*, 2001, **57**, 9225-9283.
42 K. Bougrin, A. Loupy and M. Soufiaoui, *J. Photochem. Photobiol., C: Photochemistry Reviews*, 2005, **6**, 139-167.
43 C. O. Kappe, B. Pieber and D. Dallinger, *Angew. Chem., Int. Ed.*, 2013, **52**, 1088-1094.
44 C. O. Kappe, *Angew. Chem., Int. Ed.*, 2013, **125**, 8080-8084.
45 S. Liu, M. A. Haller, H. Ma, L. R. Dalton, S. H. Jang and A. Y. Jen, *Adv. Mater.*, 2003, **15**, 603-607.
46 A. B. Marco, R. Andreu, S. Franco, J. Garín, J. Orduna, B. Villacampa and R. Alicante, *Tetrahedron*, 2013, **69**, 3919-3926.
47 L. An, Z. Cai, W. Wang, J. Pu and Z. Li, *Eur. Polym. J.*, 2014, **52**, 166-171
48 J. Casado, V. Hernández, O. K. Kim, J. M. Lehn, J. T. López Navarrete, S. Delgado Ledesma, R. Ponce Ortiz, M. C. Ruiz Delgado, Y. Vida and E. Pérez‐Inestrosa, *Chem-Eur J*, 2004, **10**, 3805-3816.